Dynamical LEED study of Pd(111)-($\sqrt{3}\times\sqrt{3}$)*R*30°-Xe

M. Caragiu,* Th. Seyller,† and R. D. Diehl‡
Physics Department, Penn State University, University Park, Pennsylvania 16802
(Received 14 June 2002; published 20 November 2002)

A low-energy electron diffraction (LEED) study of Pd(111)-($\sqrt{3}\times\sqrt{3}$)*R*30°-Xe at 77 K indicates that the Xe adsorption site is on top of the Pd atoms. The Xe–Pd bond length is 3.07 Å ± 0.06 Å. The substrate structure is essentially unrelaxed from the bulk structure. These results contrast with an earlier spin-polarized LEED study, which indicated that hollow sites are occupied in this structure. The low-coordination-site geometry for Xe on Pd(111) is discussed in the context of earlier experimental studies and recent density functional theory results for Xe adsorption on metal surfaces.

DOI: 10.1103/PhysRevB.66.195411 PACS number(s): 68.35.Bs, 61.14.Hg

I. INTRODUCTION

The physics of weakly adsorbed gases has been subject to experimental and theoretical studies for many years.[1] In these so-called physisorption systems, the primary interaction between the substrate and the adsorbate consists of the attractive van der Waals interaction and a repulsive interaction due to wave function overlap. Since the van der Waals interaction is nondirectional, the equilibrium site for physisorbed noble gases has been presumed to be a high-coordination site. This presumption has been a great hindrance to the development of accurate short-range physisorption potentials since it has delayed experiments to measure the adsorption geometries of physisorbed atoms. Although the adsorption site is an important and fundamental feature of any adsorption system, the determination of adsorption sites for adsorbed Xe has a long and convoluted history, as briefly recounted below. The dilemma is illustrated by two empirical determinations of the adsorption potential for Xe on Pt(111), both based on nonstructural experimental data. Whereas one study indicates that the top site is preferred with an interlayer spacing of 3.3 Å,[2] the other work finds that the hollow sites are preferred at an interlayer spacing of 3.1 Å.[3]

A discussion concerning the possibility that Xe might not always prefer high-coordination sites was triggered in 1990 by an analysis of He atom diffraction (HAS) data[4–6] from the uniaxially compressed phase of Xe on Pt(111), which forms at temperatures below 60 K. The diffraction intensities from this incommensurate domain-wall structure were shown to be consistent with a triangular array of preferred sites.[6] Such a triangular array is formed by the top sites, as shown in Fig. 1. The hollow sites, on the other hand, form a honeycomb array, as long as the two types of hollow sites (fcc and hcp) are degenerate. If one type of hollow site were energetically favorable, then the preferred type of hollow sites would also form a triangular array consistent with the HAS data.[7,8] However, since only a small difference in the adsorption energies of Xe in the two types of hollow sites is expected, top-site adsorption was proposed to explain the He-atom diffraction results.

An early density functional theory (DFT) local density approximation (LDA) cluster calculation[9] supported the top-site proposal. This calculation showed that the energetically favorable adsorption site is on top of the Pt atoms with a binding energy about 30 meV higher than for the hollow sites. The bond length found in this calculation was 3.0 Å, which is shorter than the hard sphere estimate of 3.54 Å.

Despite this indirect evidence that Xe occupies top sites on Pt(111), a spin-polarized low-energy electron diffraction (SPLEED) study of Pt(111)-($\sqrt{3}\times\sqrt{3}$)*R*30°-Xe (Ref. 10) indicated that the Xe atoms occupy the hollow sites. The Pt–Xe distance found in this SPLEED study was 4.2 Å, considerably longer than the hard-sphere estimate of 3.2 Å (see Table I). This result disagreed with the HAS analysis discussed above, but it was corroborated by another SPLEED study by the same group on Pd(111)-($\sqrt{3}\times\sqrt{3}$)*R*30°-Xe,[11] which also found the Xe atoms to adsorb in hollow sites. In the course of the same study the adsorption site of Xe in a disordered phase at a lower coverage was determined to be the top site. This was interpreted as being consistent with the cluster calculations because both correspond to a lower density of adsorbed Xe. The picture that emerged from the

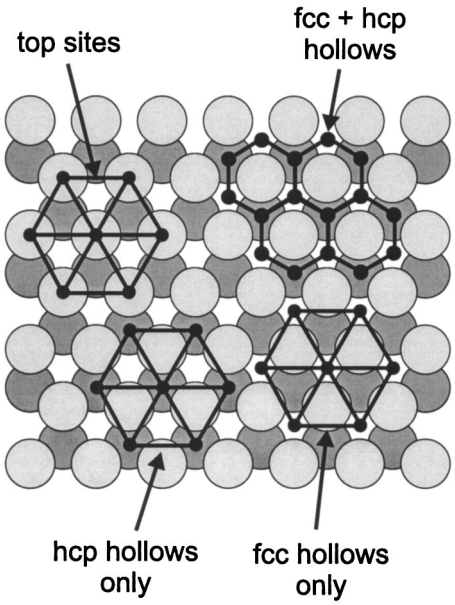

FIG. 1. Fcc (111) surface and arrays of adsorption sites. The top sites form a triangular array. Degenerate hollow sites form a honeycomb array. If only one type of hollow sites would be occupied these would also form a triangular array.

TABLE I. Summary of structure determinations for Xe on transition metal surfaces. $d_{\mathrm{Xe-M}}$ is the Xe–substrate interlayer spacing determined in these studies. The ''hard-sphere'' model predictions d_{hs} are calculated using nearest-neighbor spacings found in solids. $\Delta d = d_{\mathrm{Xe-M}} - d_{\mathrm{hs}}$ is the difference between the observed interlayer distance and the hard sphere estimate, q is the monolayer adsorption energy in meV.

System	Site	$d_{\mathrm{Xe-M}}$ (Å)	d_{hs} (Å)	Δd (Å)	q (meV)
Cu(111)-($\sqrt{3}\times\sqrt{3}$)$R30°$-Xe[a]	top	3.60 ± 0.08	3.47	$+0.13\pm0.08$	200[h]
Ag(111)-Xe-incommensurate[b]	mixed	3.55 ± 0.1	3.25–3.65	$(-0.3$ to $0.1)\pm0.1$	225[i]
Ru(0001)-($\sqrt{3}\times\sqrt{3}$)$R30°$-Xe[c]	top	3.54 ± 0.06	3.54	$+0.00\pm0.06$	230[j]
Pt(111)-($\sqrt{3}\times\sqrt{3}$)$R30°$-Xe[d]	hcp/fcc	4.2 ± 0.1	3.20	$+1.0\pm0.1$	270[k]
Pt(111)-($\sqrt{3}\times\sqrt{3}$)$R30°$-Xe[e]	top	3.4 ± 0.2	3.58	-0.18 ± 0.1	270[k]
Pd(111)-($\sqrt{3}\times\sqrt{3}$)$R30°$-Xe[f]	hcp/fcc	3.5 ± 0.1	3.20	$+0.3\pm0.1$	330[l]
Pd(111)-($\sqrt{3}\times\sqrt{3}$)$R30°$-Xe[g]	top	3.07 ± 0.06	3.56	-0.49 ± 0.06	330[l]
Pd(111)-disordered-Xe[f]	top	4.0 ± 0.1	3.56	$+0.44\pm0.1$	360[l]

[a]Reference 13.
[b]Reference 25.
[c]Reference 12.
[d]Reference 10.
[e]Reference 15.
[f]Reference 11.
[g]This work.
[h]Estimated value based on values published or similar surfaces. References 1 and 24 .
[i]Reference 26.
[j]Reference 27.
[k]Reference 1.
[l]Reference 28.

SPLEED and DFT studies is that Xe occupies top sites at low coverage and hollow sites at high coverage. The change in the adsorption site was attributed to a mutual depolarization of the Xe atoms as their density increased, and a concomitant weakening of the chemical component of the Xe–Pt bond.

This picture was upset by later low-energy electron diffraction (LEED) studies of the ($\sqrt{3}\times\sqrt{3}$)$R30°$ structures of Xe on Ru(0001) (Ref. 12) and Cu(111).[13] In both cases, Xe was found to occupy top sites, which was puzzling because the adsorption energies for these two substrates are smaller than for Pt(111) and Pd(111). Why would Xe prefer top sites in these cases but not on the stronger substrates? The weakest possible bond is the one without hybridization. If hybridization is the cause for the top-site preference, then hollow site adsorption should be expected on the weaker substrates.

A more recent study of the phonons of the commensurate ($\sqrt{3}\times\sqrt{3}$)$R30°$ structure of Xe on Pt(111) (Ref. 14) suggested that the earlier hollow site determination for Xe/Pt(111) might be erroneous. In that study, experimental data for the zone-center energy gap for the in-plane Xe vibrations were compared to model calculations, and the results strongly suggested that the experimental data were consistent with the top-site model. This particular part of the puzzle was finally resolved by a recent LEED study of Pt(111)-($\sqrt{3}\times\sqrt{3}$)$R30°$-Xe,[15] which found, contrary to the SPLEED study, that Xe occupies the top sites in the ($\sqrt{3}\times\sqrt{3}$)$R30°$ structure on Pt(111). The Xe–Pt interlayer spacing determined in this study was 3.4 Å, which fits very well into the picture drawn by the other LEED studies. The top-site preference for Xe on Pt(111) also agrees with the more indirect evidence provided by the HAS analysis discussed earlier.[6]

There remained several unresolved issues, however, including an understanding of the origin of the top site preference. In this paper, we present LEED results which show that Xe/Pd(111) also occupies top sites in the ($\sqrt{3}\times\sqrt{3}$)$R30°$ structure, thus settling the earlier question posed as to why Xe would occupy hollow sites on the strongest substrate studied, Pd(111). In the meantime, recent DFT results[16] have taken a step toward explaining the origin of the top site, and we discuss this briefly in the context of the now-consistent set of experimental results for Xe adsorption sites on metals.

II. EXPERIMENTAL AND CALCULATIONAL PROCEDURES

The experiments were carried out using a low-current video LEED system which, is described in detail elsewhere.[17] The Pd(111) sample was cleaned by repeated cycles or Ar^+ ion sputtering and annealing at 1100–1200 K. In order to reduce a possible carbon contamination of the sample surface it was annealed for prolonged periods of time in $2\cdot10^{-8}$ mbar oxygen as described in previous studies on Pd surfaces.[18,19] This procedure produced a clean and well-ordered surface as evident by Auger electron spectroscopy (AES) and LEED. Xe was adsorbed at 77 K by backfilling the chamber with Xe to a pressure of $2\cdot10^{-8}$ mbar. The adsorbed Xe gave rise to sharp superlattice spots corresponding to a well-ordered ($\sqrt{3}\times\sqrt{3}$)$R30°$ structure.

The LEED calculations were performed using the Symmetrized Automated Tensor LEED (SATLEED) package and the phase shift programs provided by Barbieri and Van Hove.[20] 12 phase shifts were used for the scattering from both the Xe and the Pt atoms. The Debye temperatures used in our analysis were 64 K for Xe and 274 K for Pd. We calculated the $I(E)$ spectra for different adsorption sites: top, fcc hollows, hcp hollows, and a mixture of fcc and hcp hol-

TABLE II. Optimum Pendry *R*-factors for different structural models tested with SATLEED. R_P is the overall *R*-factor, $R_{\rm fr}$ is the *R*-factor for the fractional order beams.

Model	R_P	$R_{\rm fr}$
Top	0.18	0.22
fcc hollows	0.47	0.75
hcp hollows	0.47	0.70
fcc+hcp (60%:40%)	0.40	0.61

lows. For each geometry, we optimized the structural parameters and nonstructural parameters in order to obtain the best fits. The agreement between experimental and theoretical spectra was tested using the Pendry *R*-factor R_P.[21] The real part of the inner potential was varied in the *R*-factor analysis, the final value being 5.4 eV. The imaginary part of the inner potential was also optimized and the best fits were obtained for a value of -6.0 eV. The experimental data set consisted of 9 symmetrically inequivalent beams with a total energy range of 3500 eV.

III. RESULTS AND DISCUSSION

Table II summarizes the best Pendry *R*-factors obtained for each adsorption geometry. As seen from this table the best agreement between the experiment and the model calculations is found for the top site. Figure 2 shows best-fit theoretical and experimental $I(E)$ curves for the top-site adsorption and for Xe adsorbed in a mixture of fcc and hcp hollow sites. Both models yield a comparable agreement for the integer order beams, evident by both visual inspection and by means of the Pendry *R*-factor (top: 0.18 and hollows: 0.21). However, the agreement for the fractional order beams is much better for the top-site model. This can be seen by visual comparison of the experimental and theoretical spectra in Fig. 2, as well as by means of the Pendry *R*-factors for the fractional order beams $R_{\rm fr}$, given in Table II.

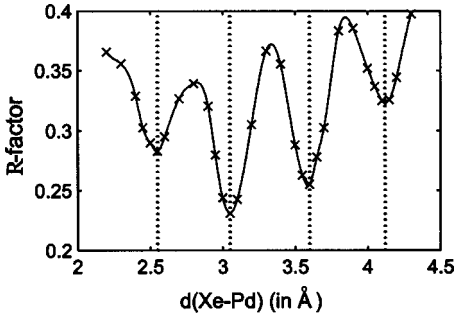

FIG. 3. Variation of the Pendry *R*-factor with the Xe–Pd interlayer spacing. Four minima are present, corresponding to interlayer spacings that differ by, roughly, multiples of 0.5 Å.

Whereas there is no doubt about the adsorption site, there was considerable difficulty to determine the exact Xe–Pd interlayer spacing due to the near-degeneracy of *R*-factor minima. The LEED calculation found a total of four minima in the *R*-factor variation with the Xe–Pd spacing. This result is not unique, since one can expect an oscillatory behavior of the reliability factor as a function of the interlayer separation, due to the restoration of the interference conditions for the reflected electron waves, once the interlayer distance equals a multiple of the electron half wavelength. In our particular case, a variation of the Xe–Pd distance with approximately 0.5 Å (and its multiples) gives structures for which minima in the *R*-factor are obtained.

Figure 3 shows the Pendry *R*-factor as a function of the Xe–Pd distance. The vertical dotted lines mark the minima that are obtained for the approximate Xe–Pd distances of

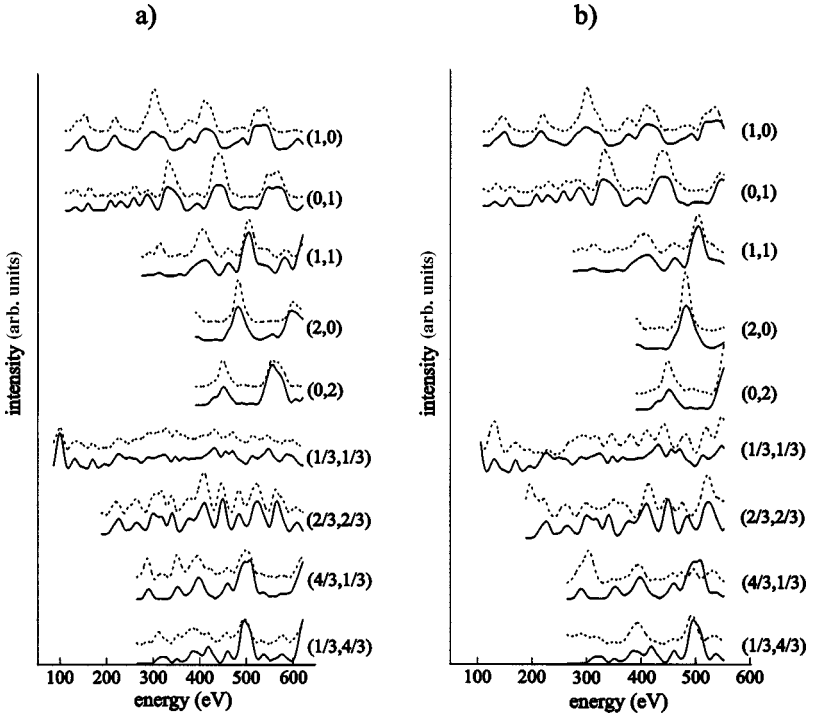

FIG. 2. Theoretical (dashed curves) and experimental (solid curves) $I(E)$ spectra for (a) top-site adsorption of Xe on Pt(111) and (b) adsorption of Xe in a mixture of 60% fcc and 40% hcp hollows. For clarity the curves are normalized to the same intensity. The calculation for the mixture of hollow sites was stopped at 550 eV because of computer limitations.

TABLE III. The Pendry *R*-factors for individual beams, corresponding to the four best-fit structures accommodating Xe atoms in top sites. The bold characters represent the lowest *R*-factor attained by each beam, as the Xe–Pd interlayer distance varies.

Beam d(Xe–Pd) (Å)	(1,0)	(0,1)	(1,1)	(2,0)	(0,2)	(1/3,1/3)	(2/3,2/3)	(4/3,1/3)	(1/3,4/3)
2.56	0.173	**0.111**	**0.102**	0.122	0.180	0.402	**0.082**	0.383	0.381
3.07	**0.128**	0.179	0.142	**0.094**	**0.114**	**0.149**	0.127	**0.305**	0.338
3.61	0.163	0.151	0.160	0.113	0.155	0.154	0.172	0.350	0.227
4.12	0.208	0.130	0.148	0.118	0.163	0.363	0.236	0.444	**0.184**

2.55 Å, 3.05 Å, 3.6 Å, and 4.1 Å. After a careful optimization of these four structures, we obtained the lowest individual Pendry *R*-factors for each of them: 0.219, 0.176, 0.181, and 0.230 for the Xe–Pd distances of 2.56 ± 0.1 Å, 3.07 ± 0.06 Å, 3.61 ± 0.06 Å, and 4.12 ± 0.08 Å, respectively.

The structures having the smallest and the largest of these four Xe–Pd distances were ruled out, primarily based on their higher *R*-factors, and also by comparison with the ''hard-sphere'' model prediction of the Xe–Pd distance of 3.56 Å (see Table I). The problem therefore was to choose between the 3.07 Å and the 3.61 Å Xe–Pd distances. Since the corresponding structures have very similar *R*-factors, we considered comparing the *R*-factors for each of the 9 inequivalent beams included in the LEED calculations. Table III lists the Pendry *R*-factors for all the beams, as obtained for each structure that presented an overall *R*-factor minimum. The structure corresponding to $d(\text{Xe–Pd}) = 3.07$ Å, exhibits the lowest possible *R*-factors for 5 out of 9 beams, whereas the $d(\text{Xe–Pd}) = 2.56$ Å structure presents lowest *R*-factors for 3 other beams. Although small, the *R*-factor values as obtained for the $d(\text{Xe–Pd}) = 3.6$ Å structure, do not contain a minimum value for any individual beam. The minimum values for the *R*-factors of each beam are highlighted in Table III. Although it would be considerably more satisfactory if there were a larger difference between the overall *R*-factors, we feel that this comparison provides some weight in favor of the 3.07 Å Xe–Pd distance. This distance is also more consistent with the hard sphere estimate, given that Xe binds more strongly to Pd(111) than to Pt(111). Performing the LEED optimization using various other *R*-factors did not give different results, nor did they make a better distinction between the two structures. Therefore we report our final result, after calculating the variance of the *R*-factor, as a Xe–Pd distance of 3.07 ± 0.06 Å, but we cannot rule out the possibility of the longer distance.

The structural parameters for the $(\sqrt{3} \times \sqrt{3})R30°$ structure found in our analysis are summarized in Fig. 4. There is also some indication of an extremely small rumpling of the substrate. The Pd atoms directly beneath the Xe atoms are pushed slightly $(0.02 \pm 0.03$ Å) toward the bulk. Although the error of this value is relatively large, we note similar rumplings have been observed for the $(\sqrt{3} \times \sqrt{3})R30°$ phases of Xe on other close-packed metal surfaces.[12,13,15] Another class of adsorption systems, where top site adsorption was unexpected but frequently observed, is alkali metals on close-packed metal surfaces.[22] In those cases where alkalis were observed in top sites, the rumpling is much more pronounced.[22] This indicates that the perturbation of the substrate due to Xe adsorption is considerably weaker than in the case of alkali metals, as expected on the basis of the adsorption strength. Figure 4 also indicates that the termination of the Pd surface is essentially bulklike—the interlayer spacing between the top-layer Pd atoms (those not occupied by Xe) and the second-layer Pd atoms is 2.27 ± 0.03 Å, while the next two interlayer spacings are 2.24 ± 0.02 Å, consistent with the bulk value. The spherically-averaged atomic vibrational amplitudes determined in this study are 0.25 Å for Xe, 0.09 Å for the first Pd layer, 0.07 Å for the second Pd layer, and 0.06 Å for all other Pd layers.

The origin of the discrepancy between the results of the present work and the SPLEED study[11] is unknown. The same is true for the SPLEED study[10] which found Xe in the hollow sites on Pt(111) in contrast to the results of our recent LEED study,[15] which indicates top-site adsorption. For Xe on Pt(111), the analysis of the SPLEED data yielded an *R*-factor minimum at a Xe–Pt spacing of 3.6 Å for the top-site.[10] The authors, however, ruled out this minimum in favor of a deeper minimum found for hollow-site adsorption. Multiple minima were also observed in the SPLEED study of Xe/Pd(111). There, the comparison between experiment and theory for two different electron energies indicated minima in the *R*-factor curves for the top site at spacings around 3.6 Å and 3.9 Å, respectively. These were disregarded because they did not occur at the same Xe–Pd interlayer spacing. However, distances smaller than 3.4 Å apparently were not tested for the top site, and the *R*-factor of the chosen hollow site structure did not differ much from those of the top site structures. Therefore the site identification in that study was somewhat ambiguous in any case.

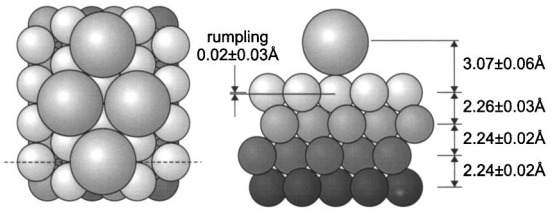

FIG. 4. Best fit model for the $(\sqrt{3} \times \sqrt{3})R30°$ structure of Xe on Pd(111). The Xe atoms adsorb in on-top positions. The dashed line on the left-hand side indicates the cut through the structure shown on the right-hand side. The termination of the Pd(111) crystal is essentially bulklike. The Pd atoms directly under the Xe atoms are pushed slightly toward the bulk. (Drawing is not to scale.)

As can bee seen from Table I, the Xe–metal bond lengths are close to the hard sphere estimates for Cu(111) and Ru(0001), the substrates with the weakest binding. For the other two substrates Pt(111) and Pd(111) the bond lengths are considerably smaller than the hard sphere estimates, indicating a trend towards smaller bond length with increasing bond strength. This is corroborated by recent DFT calculations for Xe adsorption on Cu(111), Pt(111), and Pd(111),[16] which also concur that the top-site structure is preferred for Xe on these surfaces and that the bond length is shorter for stronger adsorption.

The Pd, Pt, and Cu substrates are all transition metals, for which it is known that the free electron theory breaks down most seriously. The *d* valence orbitals are more contracted than the valence *s* and *p* orbitals, and therefore do not overlap so strongly. The result is a narrower band, which is more identifiable to its atomic orbital character than with the simple metals. For this reason, one can refer to the occupation of various *d* orbitals to explain the interaction of Xe atoms with the substrate. In the case of Xe/Pd(111), the DFT study shows[16] that there is a change in the electron charge density of both adsorbate and substrate upon adsorption. This takes the form of a depletion of electron density on the Xe atom (mainly Xe p_z orbitals) and a decrease in the occupation of Pd d_{z^2} for the substrate atoms closest to the Xe atoms. The same effect, although smaller, is seen for Xe on Pt(111), and the effect is even smaller on Cu(111).

In explaining the preference for Xe to sit in the top adsorption sites, it is argued that the Xe p_z orbitals interact with the unoccupied components of the *d* shell corresponding to the substrate atoms underneath. Conversely, in a hollow site, the Xe p_z orbitals would be closer to the occupied d_{xy}, d_{yz}, d_{xz}, and components of the *d* shell. Therefore, aside from the spatial symmetry of these particular orbitals, the relative electron occupation of those *d* shell components may make the hollow site less favorable due to Pauli repulsion. The calculated binding energy of Xe on Pt as a function of vertical distance for the top and fcc sites[16] shows that the top site absorption corresponds to stronger binding for any adsorbate-substrate distance. Being less repelled by the substrate atoms when in top position, the Xe atoms are predicted to sit closer to the surface when in the top site as compared to the fcc site. While this latter prediction cannot be experimentally verified by this experiment since all Xe atoms are in the same (top) site, the same phenomenon had been predicted earlier for Ar adsorption on Ag(111).[23]

IV. CONCLUSIONS

In the paper at hand we have presented a dynamical LEED study of Pd(111)-($\sqrt{3}\times\sqrt{3}$)$R30°$-Xe which indicates that Xe adsorbs in the top sites. The Xe–Pd bond length is 3.07 ± 0.06 Å and the substrate termination is essentially bulk like. Our results fit well to results of three other LEED studies of Xe on close-packed metal surfaces but are in contradiction to an earlier SPLEED study of the same structure, which indicated that Xe prefers the hollow sites. The LEED studies, however, indicate that adsorption of Xe in top sites seems to be a common phenomenon and recent DFT calculations concur with this conclusion. Those studies suggest that the top site preference arises not directly as a result of the increased chemical attraction of the top site, but mainly as a result of the decreased Pauli repulsion in the top site compared to the hollow site, due to the relative orbital symmetries. The extent of this preference, in terms of range of adsorbate gases and substrates for which it exists, is not yet known because there has not yet been a clear experimental observation of a rare gas adsorbed in a hollow site. Thus, the topic of Xe adsorption on metal surfaces requires more experimental and theoretical studies in order to elucidate the phenomenon of top-site adsorption.

ACKNOWLEDGMENTS

We would like to thank L. W. Bruch, P. Zeppenfeld, J. F. Annett, M. Scheffler, C. Stampfl, P. A. Dowben, and D. M. Eigler for many enlightening communications. We also thank Michael Hochstrasser and Roy Willis for providing the Pd(111) crystal. This work was supported by the NSF DMR-9629715 and DMR-9819977.

*Current address: Department of Physics, Ohio Northern University, South Main Street, Ada, Ohio 45817. Electronic address: m-caragiu@onu.edu

†Current address: Institut für Technische Physik II, Universität Erlangen-Nürnberg, Erwin-Rommel-Straße 1, 91058 Erlangen, Germany. Electronic address: thomas.seyller@physik.uni-erlangen.de

‡Author to whom correspondence should be addressed. Electronic address: rdiehl@psu.edu

[1] L. W. Bruch, M. W. Cole, and E. Zaremba, *Physical Adsorption: Forces and Phenomena* (Oxford University Press, Oxford, 1997).

[2] J. A. Barker, C. T. Rettner, and D. S. Bethune, Chem. Phys. Lett. **188**, 471 (1992).

[3] P. A. Rejto and H. C. Andersen, J. Chem. Phys. **98**, 7636 (1993).

[4] P. Zeppenfeld, K. Kern, R. David, and G. Comsa, Phys. Rev. B **38**, 3918 (1988).

[5] K. Kern, R. David, P. Zeppenfeld, and G. Comsa, Surf. Sci. **195**, 353 (1988).

[6] J. M. Gottlieb, Phys. Rev. B **42**, 5377 (1990).

[7] P. Zeppenfeld, G. Comsa, and J. A. Barker, Phys. Rev. B **46**, 8806 (1992).

[8] K. Kern, R. David, P. Zeppenfeld, R. Palmer, and G. Comsa, Solid State Commun. **62**, 391 (1987).

[9] J. E. Müller, Phys. Rev. Lett. **65**, 3021 (1990).

[10] M. Potthoff, G. Hilgers, N. Müller, U. Heinzmann, L. Haunert, J. Braun, and G. Borstel, Surf. Sci. **322**, 193 (1995).

[11] G. Hilgers, M. Potthoff, N. Müller, and U. Heinzmann, Surf. Sci. **322**, 207 (1995).

[12] B. Narloch and D. Menzel, Chem. Phys. Lett. **270**, 163 (1997).

[13] T. Seyller, M. Caragiu, R. D. Diehl, P. Kaukasoina, and M. Lindroos, Chem. Phys. Lett. **291**, 567 (1998).

[14] L. W. Bruch, A. P. Graham, and J. P. Toennies, Mol. Phys. **95**, 579 (1998).

[15] T. Seyller, M. Caragiu, R. D. Diehl, P. Kaukasoina, and M. Lindroos, Phys. Rev. B **60**, 11 084 (1999).
[16] J. L. F. Da Silva, C. Stampfl, and M. Scheffler, Phys. Rev. Lett. (submitted).
[17] G. S. Leatherman, R. D. Diehl, P. Kaukasoina, and M. Lindroos, Phys. Rev. B **53**, 10 254 (1995).
[18] N. Otha, Y. Ohno, and T. Matsushima, Surf. Sci. **276**, L1 (1992).
[19] A. Berkó and F. Solymosi, Surf. Sci. **187**, 359 (1987).
[20] A. Barbieri and M. A. Van Hove (personal communication).
[21] J. B. Pendry, J. Phys. C **13**, 937 (1980).
[22] R. D. Diehl and R. McGrath, Surf. Sci. Rep. **23**, 43 (1996).
[23] L. W. Bruch, Phys. Rev. B **64**, 033407 (2001).
[24] G. Vidali, G. Ihm, H.-Y. Kim, and M. W. Cole, Surf. Sci. Rep. **12**, 133 (1991).
[25] J. Unguris, L. W. Bruch, E. R. Moog, and M. B. Webb, Surf. Sci. **87**, 415 (1979).
[26] J. Unguris, L. W. Bruch, E. R. Moog, and M. B. Webb, Surf. Sci. **109**, 522 (1981).
[27] H. Schichting and D. Menzel, Surf. Sci. **272**, 27 (1992).
[28] K. Wandelt and J. E. Hülse, J. Chem. Phys. **80**, 1340 (1984).